

Adaptive observer-based optimum tracking control design for the suppression of stick-slip and bit-bounce oscillations in drilling systems

Mejbahul Sarker

Abstract - Oilwell drillstring sometimes vibrate severely and can twist off in hard rock drilling. There are many reasons for drillstring failure, such as vibration, fatigue, and buckling. Stick-slip particularly predominates when drilling with polycrystalline diamond compact (PDC) bits, which may also excite severe axial and lateral vibrations in the bottom hole assembly, causing damage to the drillstrings and downhole equipment. Controlling these vibrations is essential to improving the efficiency and minimizing the cost of drilling. An adaptive observer for estimation the axial and torsional vibrations through the drillstring has been developed for stick-slip and bit-bounce detection. A bond graph model of a drillstring has been developed that predicts axial vibration, torsional vibration, and coupling between axial and torsional vibration due to bit-rock interaction. Axial and torsional submodels use a lumped-segment approach, with each submodel having a total of 21 segments to capture vibration of the kelly, drill pipes, and drill collars. In addition, the model incorporates viscous damping, hydrodynamic damping, and hydraulic forces due to drilling mud; an empirical treatment of rock-bit interaction, and top drive dynamics. The model predicts the expected coupling between weight on bit (WOB), bit speed, and rock-bit interaction conditions; and their effect on stick-slip. Mitigation open-loop measures used in the drilling industry (increasing rotary speed and decreasing WOB through changing derrick tension) were applied to the model, and successfully eliminated stick-slip. This paper addresses the advantages of a linear quadratic regulator (LQR) controller, compared to a spring-damper isolator, for stick-slip and bit-bounce mitigation in an oilwell drillstring. The model, implemented using the bond graph formalism, is a useful tool for design and sensitivity analysis due to its physically meaningful parameters and low simulation times on a personal computer.

Keyword: Drilling, vibration, adaptive observer lumped-segment model, stick-slip, bit-bounce, bit-rock interaction, linear quadratic regulator, torsion spring-damper.

Mejbahul Sarker^{*} Lecturer, Department of Petroleum Engineering, American University of Kurdistan.

I. INTRODUCTION

The boreholes of oil exploration and exploitation wells are typically drilled by means of a rock cutting tool (drill bit), which is attached at the end of a rather long drill string consisting of many smaller interconnected drillpipe sections, and driven by a speed controlled electrical drive. Due to large lengths and small cross sections of the drilling pipes, low tool inertia, and emphasized tool vs. rock bed friction, the overall drillstring electrical drive is prone to poorly damped torsional vibrations including stick-slip behavior. Stick-slip predominates when drilling with drag bits (especially with PDC bits) and stick-slip oscillations induce large cyclic stresses, which may also excite severe axial and lateral vibrations in the bottom hole assembly (BHA). This can lead to fatigue problems, reduction of bit life, unexpected changes in drilling direction, and even failure of the drillstring. Since drilling is one of the most expensive operations in oil exploration and development, vibration control in the oil drilling process is required from an economic point of view.

In practice, the drilling operator typically controls the surface-controlled drilling parameters, such as the weight on bit (WOB), drilling fluid flow through the drill pipe, the drillstring rotational speed and the density and viscosity of the drilling fluid to optimize the drilling operations. In particular, the only means of controlling vibration with current monitoring technology is to change either the rotary speed or the weight on bit. Historically, the experience of drillers has revealed that increasing the rotary speed, decreasing the weight on bit, modifying the drilling mud characteristics and introducing an additional friction at the bit etc. are effective strategies to suppress stick-slip motion [1-11]. Trade-offs must be managed, however. For example, mitigating stick-slip by reducing weight on bit might result in a lower rate of penetration. Increasing rotary speed to reduce stick-slip might bring

other vibration modes into resonance. The effectiveness of ad hoc changing of drilling parameters is also dependent on the skill of the operator. Recently linear quadratic regulator controllers have been discussed [1, 3] as a means of improving multiple types of vibration such as stick-slip and bit-bounce motion simultaneously.

This paper is organized as follows. Section 2 develops a lumped-segment drillstring model, with coupled axial and torsional vibratory motions, that will allow the simulation to accurately capture the stick-slip and bit-bounce. In Section 3, a linear quadratic regulator (LQR) has been designed to control the torsional dynamics of the system. An alternative control schemes called soft torque rotary system (STRS) is discussed in Section 4. In Section 5, the complete drillstring model is used to study the theoretical performance of the LQR controller compared with torsion spring-damper (or virtual spring-damper as in the STRS system) on the mitigation of stick-slip and bit-bounce vibrations. The advantages of LQR controller over torsion spring-damper has been discussed in Section 6. Conclusions and future work are given in Section 7. The model is a potentially valuable tool in the design of drillstrings with optimized top drive speeds, stabilizer and downhole tool locations, mud motor speeds, and trajectories. The model development was facilitated by the bond graph approach, an overview of which is given in Appx. A.

II. OILWELL DRILLING SYSTEM MODELING

Several dynamic formulations have been reported for investigating specific aspects of drillstring vibrational behavior and few of them have tackled stick-slip. One of the major difficulties in modeling stick-slip stems from the inaccurate description of some involved parameters and downhole boundary conditions. Leine *et al.* [2] presented a stick-slip whirl model which consists of a submodel for the whirling motion and a submodel for the stick-slip motion. The stick-slip whirl model was a simplification of drilling confined in a borehole with drilling mud. Their model was a low-dimensional model and it aimed at explaining the basic nonlinear dynamic phenomena observed in downhole experiments. The model system was analyzed with the discontinuous bifurcations method which indicates physical phenomena such as dry friction, impact and

backlash in mechanical systems or diode elements in electrical circuits which are often studied by means of mathematical models with some kind of discontinuity. The disappearance of stick-slip vibration when whirl vibration appears was explained by bifurcation theory. Stick slip was prevalent at low angular velocity and backward whirl was prevalent for high angular velocity consistent with the measurements. They did not consider the effect of axial vibration and rock-bit interaction in the model.

Christoforou and Yigit [3,4] used a simple dynamic model to simulate the effects of varying operating conditions on stick-slip and bit bounce interactions. The equations of motion of such a system were developed by using a simplified lumped parameter model with only one compliance. This model did not account for the effect of higher modes, the flow inside and outside the drillpipe and collars, or complicated cutting and friction conditions at the bit/formation interface.

Richard *et al.* [5,6] studied the self-excited stick-slip oscillations of a rotary drilling system with a drag bit, using a discrete model which takes into consideration the axial and torsional vibration modes of the bit. Coupling between these two vibration modes took place through a bit-rock interaction law which accounted for both frictional contact and cutting processes at the bit-rock interface. The cutting process introduced a delay in the equations of motion which was ultimately responsible for the existence of self-excited vibrations, exhibiting stick-slip oscillations under certain conditions. One of the limitations of their model is that the simulation stops when the bit lifts off. Furthermore, their model reduced the drillstring to a two degree of freedom system and they were working to capture more modes of vibration.

Sampaio *et al.* [7] presented a geometrically non-linear model to study the coupling of axial and torsional vibrations on a drill string, which is described as a vertical slender beam under axial rotation. The geometrical stiffening is analyzed using a non-linear finite element approximation, in which large rotations and non-linear strain displacements are taken into account. The effect of structural damping and a non-linear bit torque are considered in the model.

Navarro-Lopez and Cortes [8] presented a lumped-parameter segment model of the torsional behavior of the drillstring including the bit-rock interaction. Friction between the pipes and the borehole is neglected which means both are assumed as a vertical and

straight. The lateral bit motion was neglected in the bit-rock interaction model. The drilling mud was simplified by a viscous-type friction element at the bit.

Zamanian *et al.* [9] presented a discrete model of the drillstring which includes a rotary table at the top with torsional degrees of freedom, a BHA with torsional and axial degrees of freedom and an interaction law between the rock and drag bit. In more details, it was assumed that drill collar and bit behave as a rigid body and the moment of inertia of the drill pipe was ignored in comparing with the moment of inertia of the rotary table and BHA.

Recently Khulief *et al.* [10] formulated a finite element dynamic model of the drillstring including the drill pipes and drill collars. The model accounted for the torsional-bending inertia coupling and the axial-bending geometric nonlinear coupling. In addition, the model accounted for the gyroscopic effect, the effect of the gravitational force field, and stick-slip interaction forces. Complex modal transformations were applied and reduced-order models were obtained. The finite element formulation was then integrated into a computational scheme for calculating the natural frequencies of the whole drillstring. The computational scheme was extended further to integrate the equations of motion, either in the full-order or the reduced-order form, to obtain the dynamic response. MATLAB™ was used as a simulation tool. They did not consider hydrodynamic damping, due to drilling fluid circulation in the drill pipe and the annular space, in their model. Stick-slip interaction was giving a coupling between axial and torsional vibration but [10] did not have any discussion about the complex effect of bit rotary speed and threshold force on torque on bit.

At present, some models are available for analyzing drillstring vibrations, but none of them reflect the actual downhole conditions in drilling operations. A more relevant model should be developed to consider the combined effect of at least axial and torsional

vibration modes. Much previous work on drillstring stick-slip was based on a single degree of freedom torsional pendulum, wherein a rigid body with constant mass and moment of inertia was used to model the BHA, and a linear spring to model the drillstring. Although some previous models provided limited insight into stick-slip and bit-bounce phenomena, the continuum nature of the drillstring has been ignored.

The system being modeled consists of drill pipes, the drill collar assembly (made up of heavier collar pipes), the drill bit at the end of the collar assembly and the rock (formation). Drilling fluid is circulated in the drill pipe and the annular space between the drill pipe and the well bore. The drilling fluid is characterized by the flow rate developed by the mud pumps. The top of the drillstring is subject to a tension force, applied through the surface cables. Rotary motion is applied by an armature-controlled motor, through a gearbox, to the rotary table via the kelly (a square, hexagonal or octagonal shaped tubing that is inserted through and is an integral part of the rotary table that moves freely vertically while the rotary table turns it). In this study, a DC motor with winding inductance and resistance is assumed. The essential components of the oilwell drilling system and the necessary geometry used for the model are shown in Fig. 1. A lumped-segment approach is used in the longitudinal and torsional motion models. In the lumped segment approach, the system is divided into a series of inertias, interconnected with springs. The accuracy of the model depends on the number of elements considered; however, in contrast to a modal expansion approach, the analytical mode shapes and natural frequencies need not be determined. If a system model is divided into a larger number of elements, then the accuracy of the results will be higher. The behavior will approach that of a continuous system as the number of segments approaches infinity. A physical schematic of the lumped segment models is shown in Fig. 2.

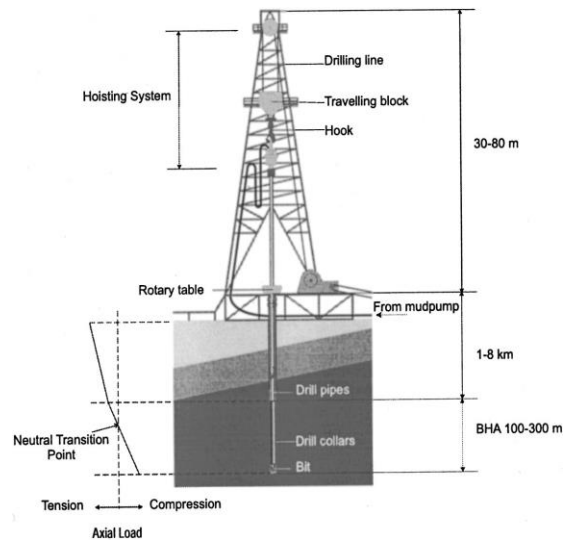


Figure 1: Oilwell drilling system (adapted from [1])

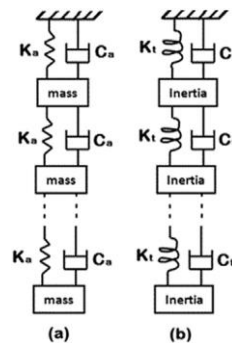


Figure 2: Physical schematic of (a) axial segments and (b) torsional segments.

a. Modeling of axial and torsional dynamics

The model accounts for the effect of drilling fluid circulation in the drillstring and the annular space between the drillstring and the wellbore, on drillstring motions. The drilling fluid was characterized by the flow rate developed by the mud pumps. Nonlaminar Newtonian flow formulations are used in calculation of fluid drag/force/damping for the longitudinal motion. Hydrodynamic damping due to drilling fluid circulation in the drillstring and the annular space was considered in the longitudinal direction instead of viscous damping. In the case of torsional motion, the viscous damping which results from the contact between drillstring surfaces and the drilling fluid was considered. In addition, the model considers the self-weight effect and buoyancy effect due to drilling fluid. Fig. 3 shows the schematic of drillstring axial segment model with the FBD of axial and torsional segments of drillstring. The terms V_p and V_a in the figures indicate drilling mud velocity inside the drillstring and the

annulus, respectively. The reader is referred to Appx. B for the equations of the fluid drag forces and rotational fluid friction to the drillstring motions. A bond graph model for longitudinal and torsional motions of a drillstring segment is shown in Fig. 4. The axial segment bond graph shows a mass (I element) and gravity force source (Se element) associated with segment velocity v . Hydrodynamic dissipative forces (R elements) also contribute to Newton's Second Law of the mass, with the flow sources (Sf) and 0-junctions calculating relative fluid flow velocities inside and outside the pipe. The dissipative forces are functions of these relative velocities. Axial compliance and material damping of the segment are modeled by parallel compliance (C) and dissipative elements, the forces of which are functions of the relative velocity (calculated by the 0-junction) of the segment with respect to the adjoining segment. The buoyancy weight of the drillstring segment acts in the longitudinal direction for the case of vertical drilling. A total of 21 segments are

used in the dynamic model to capture the first eight axial natural frequencies of the whole drillstring. One

segment is used for the relatively short kelly. For both drill pipe and collar, 10 segments are used in the model.

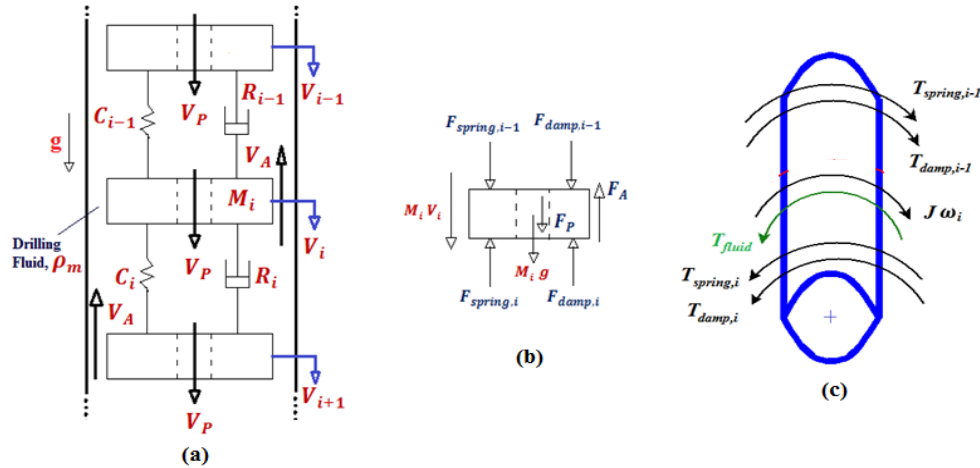


Figure 3: Schematic of (a) drillstring axial lumped segment model showing drilling fluid flow and (b) FBD of axial segment and (c) torsional segment of a vertical drillstring.

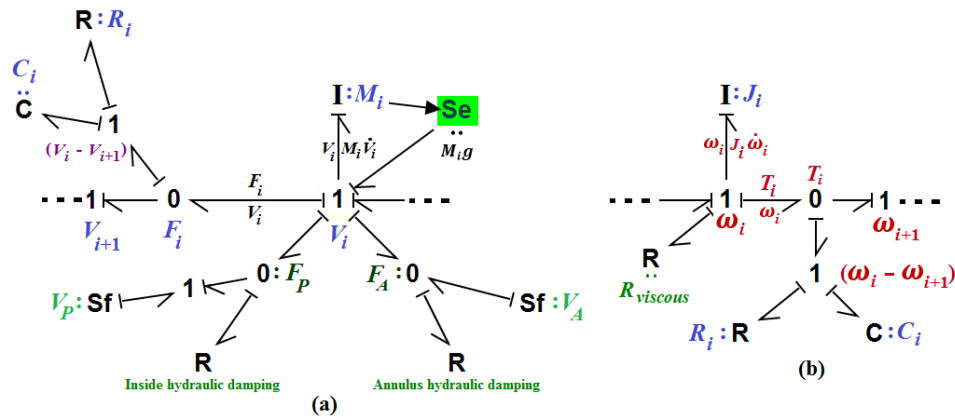


Figure 4: Bond graph segment model for (a) longitudinal (or axial) and (b) torsional motions of a vertical drillstring.

b. Coupling between axial and torsional dynamics

The bit-rock interaction provides coupling between axial and torsional drillstring dynamics. In this present work a quasi-static rock-bit model is used instead of a computationally intensive and difficult-to-parameterize complete dynamic representation. Yigit and Christoforou [3,4] have shown a static rock-bit interaction model in a drillstring represented using only two inertias and one compliance for both axial and torsional vibration. Their model is modified as described below. The original model in [4] assumed both friction and cutting torque regardless of whether or not dynamic weight on bit was sufficient to create

penetration and cuttings. Depth of cut was a function of average rather than instantaneous rotation speed, along with rate of penetration. Rate of penetration was a function of average rotation speed and a constant applied weight on bit (WOB), rather than dynamic weight on bit. This paper incorporates threshold force and the effect of instantaneous WOB and bit rotation speed on cutting torque on bit (TOB). Below a threshold force W_{fs} , the drill tool does not penetrate into the rock, leaving only friction as a source of TOB. The model equations are presented in two parts. First, the dynamic WOB, which is the axial force applied at the bit under dynamic conditions is given as in [4]

$$WOB = \begin{cases} k_c(x - s) & \text{if } x \geq s \\ 0 & \text{if } x < s \end{cases} \quad (1)$$

where k_c and s indicate formation contact stiffness and bottom-hole surface profile. Surface profile is given as [4]

$$s = s_0 f(\phi) \quad (2)$$

The formation elevation function $f(\phi)$ is chosen to be sinusoidal as in [4], $f(\phi) = \sin b\phi$, where b indicates bit factor which depends on the bit type. The term ϕ indicates rotational displacement of the bit.

The total torque on bit (TOB) is related to frictional and cutting conditions, and dynamic WOB. When bit rotary speed is in the positive direction then TOB can be written as

$$TOB = \begin{cases} TOB_f + TOB_c & WOB > W_{fs} \\ TOB_f & WOB \leq W_{fs} \end{cases} \quad (3)$$

In the case of zero bit rotary speed

$$TOB = \begin{cases} TOB_c & WOB > W_{fs} \\ 0 & WOB \leq W_{fs} \end{cases} \quad (4)$$

Finally for negative bit rotary speed

$$TOB = TOB_f \quad (5)$$

where TOB_f and TOB_c represent frictional and cutting torque on bit and both are calculated as below,

$$TOB_f = (WOB)r_b\mu(\dot{\phi}) \quad (6)$$

$$TOB_c = (WOB)r_b\xi\sqrt{\frac{\delta_c}{r_b}} \quad (7)$$

The term $\dot{\phi}$ indicates instantaneous bit rotary speed, and the function $\mu(\dot{\phi})$ characterizes the friction process at the bit and it is given as [4]

$$\mu(\dot{\phi}) = \mu_0 \left(\tanh \dot{\phi} + \frac{\alpha\dot{\phi}}{(1+\beta\dot{\phi}^2\gamma)} + \nu\dot{\phi} \right) \quad (8)$$

where μ_0 , α , β , γ , and ν are the experimentally determined parameters of the frictional model. In equation (7) the terms r_b and δ_c indicate bit radius and depth of cut per revolution, the latter given as

$$\delta_c = \frac{2\pi ROP}{\dot{\phi}}$$

(9)

The instantaneous rate of penetration (ROP) is a function of dynamic WOB, instantaneous bit speed $\dot{\phi}$, and rock/bit characteristics. The modified ROP equation from [4] can be written as

$$ROP = C_1 WOB \sqrt{\dot{\phi}} + C_2$$

(10)

where ξ , C_1 and C_2 characterize the cutting action at the bit and depend on the type of the bit and formation.

The bond graph model of the rotary drillstring is shown in Appendix C. The reader is referred to [13] for more details on the bond graph modeling method.

III. CONTROLLER DESIGN

A linear quadratic regulator (LQR) has been designed to control the torsional dynamics of the system. LQR is well-known design technique that provides optimal feedback gains. In order to determine LQR gains, a performance index is required. A performance index is the integral over time of several factors which are to intended to be minimized. The riccati equation is solved to calculate optimal linear gains. In order to reduce the dimension of the state vector and to minimize the number of states that must be physically measured or estimated, a simplified lumped parameter torsional model (Fig. 5) is used instead of taking 21 segments. The state space equation of the simplified model in Fig. 5 is

$$\dot{X} = AX + BV_c$$

(11)

where X , A , and B are the state vector, coefficient, and input matrices, respectively:

$$A = \begin{bmatrix} -\frac{R_m}{L} & 0 & -\frac{nK_m}{L} & 0 & 0 \\ 0 & 0 & 1 & 0 & 0 \\ \frac{nK_m}{J_k+J_{rt}+n^2J_m} & 0 & \frac{-c_{rt}}{J_k+J_{rt}+n^2J_m} & \frac{-K_t}{J_k+J_{rt}+n^2J_m} & 0 \\ 0 & 0 & 1 & 0 & -1 \\ 0 & 0 & 0 & \frac{K_t}{J} & \frac{-c_v}{J} \end{bmatrix}$$

(12)

$$X^T = [I \ \phi_{rt} \ \dot{\phi}_{rt} \ (\phi_{rt} - \phi) \ \dot{\phi}]$$

(13)

$$B^T = [\frac{1}{L} \ 0 \ 0 \ 0 \ 0]$$

(14)

The main goal here is not to place the new closed loop poles at an exact specified location at any cost, but to minimize the vibration state variables and the control effort. The control problem is to find out the necessary gain vector $[K]$ that will minimize the following performance index [3]:

$$C = \frac{1}{2} \int_0^{\infty} (x^T Q x + r V_c^2) dt \quad (15)$$

where Q is a weighting matrix chosen to reflect the relative importance of each state and r is a weighting factor to adjust the control effort. If the desired state vector is x_d then the resulting optimal control input (rotary table motor voltage) can be written as

$$V_c = V_{ref} - K(x - x_d) \quad (16)$$

The gain matrix, K can be written as

$$K = r^{-1} B^T P \quad (17)$$

where P is the symmetric, positive-definite solution matrix of the algebraic Riccati equation given by

$$A^T P + P A - r^{-1} P B B^T P + Q = 0 \quad (18)$$

where

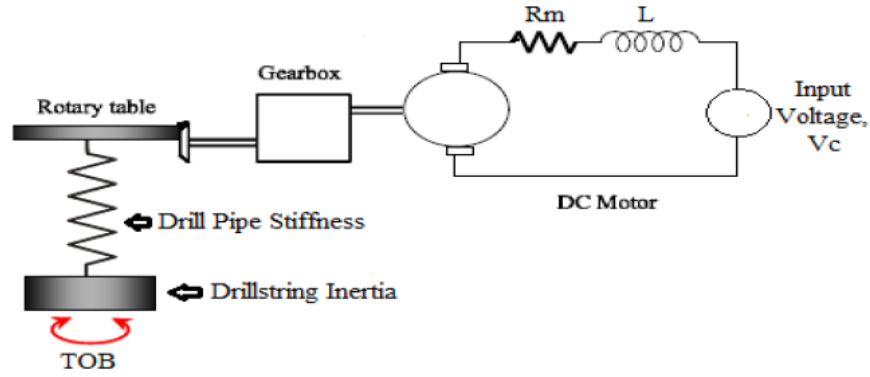
$$R = 950 \quad (19)$$

$$Q = \begin{bmatrix} 1 & 0 & 0 & 0 & 0 \\ 0 & 20000 & 0 & 0 & 0 \\ 0 & 0 & 1 & 0 & 0 \\ 0 & 0 & 0 & 80000 & 0 \\ 0 & 0 & 0 & 0 & 950000 \end{bmatrix} \quad (20)$$

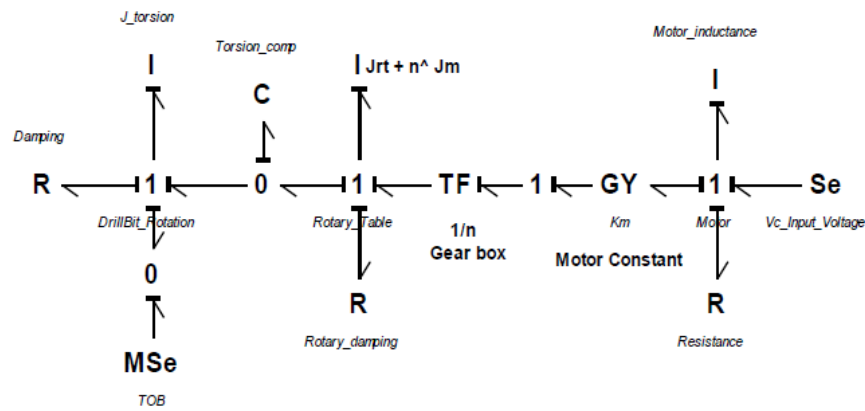
The resulting controller gains are then applied to the high order model for simulation. Fig. 6 shows the controller block diagram connection to the bond graph plant model. The control voltage necessary to keep the torsional vibrations zero while maintaining a desired bit and rotary table speed is give by

$$V_c = V_{ref} - K_1 I - K_2 (\phi_{rt} - \omega_d * t) - K_3 (\dot{\phi}_{rt} - \omega_d) - K_4 (\phi_{rt} - \phi) - K_5 (\dot{\phi} - \omega_d) \quad (19)$$

For different drilling depths the gain matrix K is calculated by using MATLAB™ and the gains vs. depth curves are shown in Fig. 7.



(a)



(b)

Figure 5: (a) Physical schematic of model used for control design. (b) Bond graph torsional model using simplified lumped parameter model

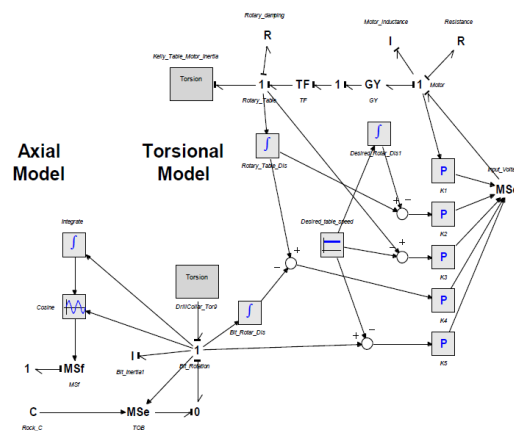


Figure 6: LQR controller block diagram connection to the bond graph plant model.

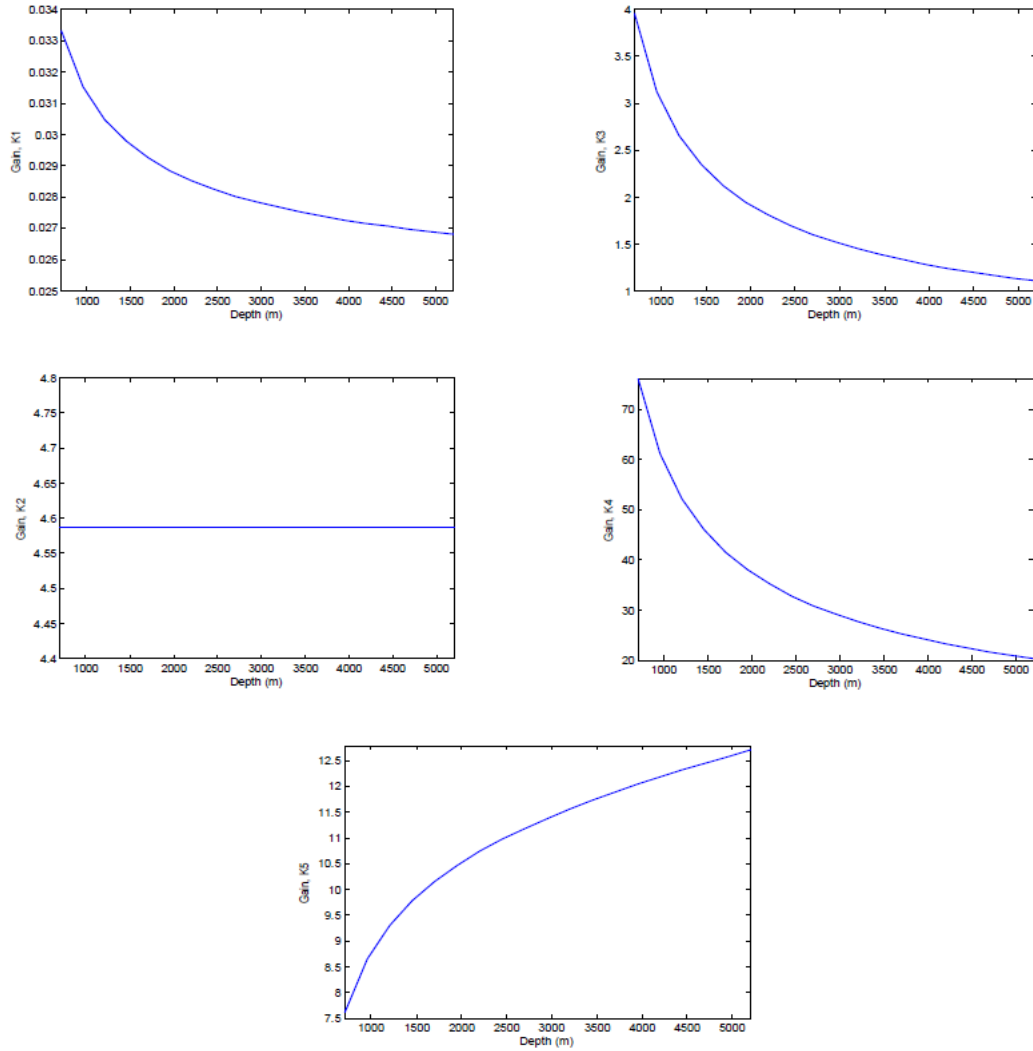


Figure 7: Gains vs. depth curves for LQR controller

IV. ALTERNATIVE CONTROL SCHEMES

In the literature, numerous solutions have been presented to control stick-slip oscillations, such as robust μ -synthesis controller [14], H_∞ controller [15], genetic algorithm optimized controller [16], D-OSKIL controller [17], torque estimator-based controller [18], and modeling error compensation based controller [19]. Many such controllers have practical limitations. However, one system that has achieved real-world acceptance is the soft torque rotary system (STRS) [20-22]. STRS is a torque feedback at the top of the drillstring which makes the system behave in a “softer” way rather than as a fixed heavy flywheel, so that the torsional waves arriving at the surface are absorbed,

breaking the harmful cycling motion. The STRS increases the system damping to the extent that rotational speeds will not drop to levels where there is a risk of the bottom hole assembly (BHA) sticking. Therefore, the feedback system, which acts on the rotary drive’s speed input, modifies the speed of the motor such that the vibrational energy is optimally extracted from the drillstring. The effect of this feedback circuit, in practice fully implemented by electronics, is to emulate a parallel combination of a torsional spring and damper in series with an ideal motor as shown in Fig. 8.

The STRS must be tuned by giving values of K_s (drive stiffness in Nm/rad) and C_s (drive damping in Nms/rad) [21]. The parameters must change as the

The current simulations study the theoretical performance of an LQR controller compared to a torsional spring-damper (or virtual spring-damper as in the STRS system) on the mitigation of stick-slip and bit-bounce vibrations in an oilwell drillstring. The simulation results for a drilling depth 4200 m, where drill pipe and collar lengths are 4000 m and 200 m, are shown below in Figs. 10-13.

Fig. 10 shows the full model simulation results in the case of conventional drilling when the desired rotary table speed is 15 rad/sec (142 rpm) with 175 kN applied WOB. Though the motor appears to maintain the rotary table speed as desired, the bit experiences large speed fluctuations indicative of stick-slip. Also, at the same time the torque at surface experiences large fluctuations consistent with stick-slip [21,22]. When the input torque grows sufficiently to overcome static friction and the bit releases, bit speed approaches the axial vibration critical speed range that is discussed in [1]. Bit-bounce then occurs as demonstrated in Fig. 10 where dynamic WOB periodically becomes zero.

Fig. 11 shows the response of the model when LQR control is activated at the simulation time of 40

seconds, for the case of 175 kN applied WOB and a desired speed of 15 rad/sec (142 rpm). As can be seen, when LQR controller is active the stick-slip vibration is controlled and a smooth drilling condition is achieved. That means the drill bit is rotating with constant desired speed and the torque at the surface becomes constant. At the same time the controller eliminates high dynamic force and bit-bounce, as a result of the axial-torsional coupling at the bit-rock interface.

Fig. 12 shows the response of the model when a torsional spring-damper system is used, for the case of 175 kN applied WOB and a desired speed of 15 rad/sec (142 rpm). The torsional spring-damper system with the assigned parameters should be unable to eliminate stick-slip vibration at the desired speed. By increasing the desired speed to 24 rad/sec (230 rpm) in Fig. 13, the torsional spring-damper system becomes able to eliminate stick-slip vibration.

From the simulation results in Fig.10-13, an LQR controller can suppress stick-slip vibrations at lower desired speeds than can a torsional spring-damper system. This indicates a theoretical advantage of an LQR controller over torsional spring-damper isolators.

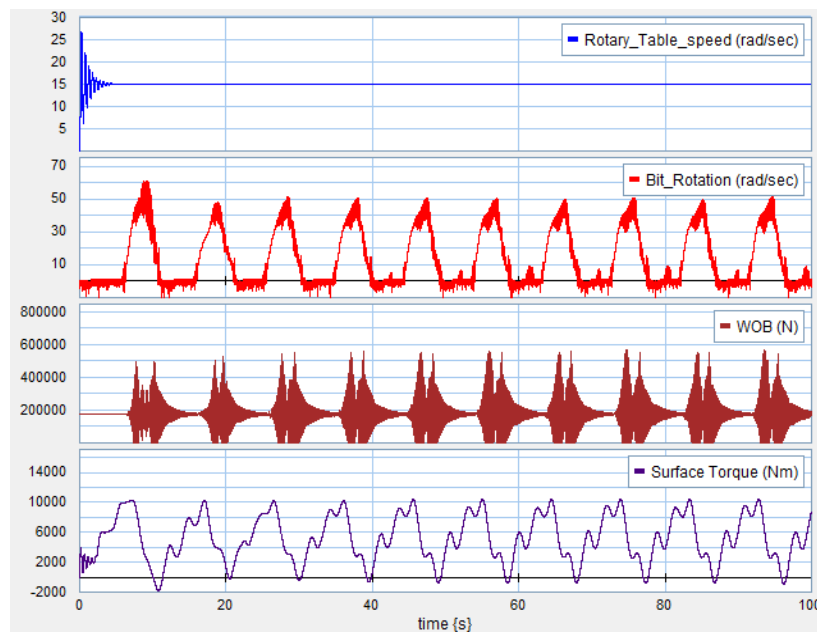


Figure 10: High stick-slip vibrations with bit-bounce at 15 rad/sec (142 rpm) rotary table speed and 175 kN applied WOB

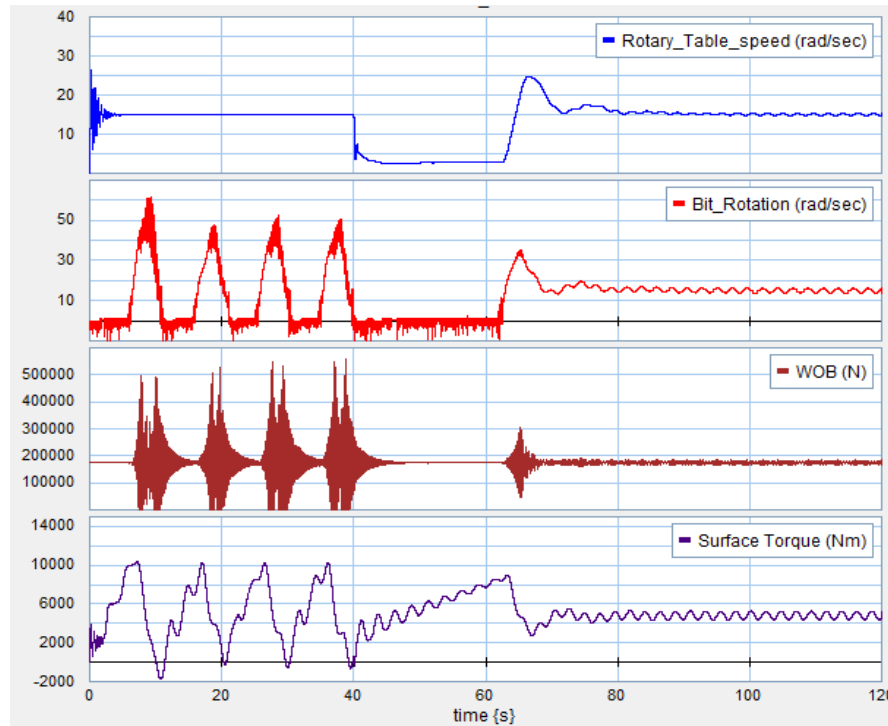


Figure 11: Stick-slip and bit-bounce eliminated by LQR control at 15 rad/sec (142 rpm) table speed and 175 kN applied WOB

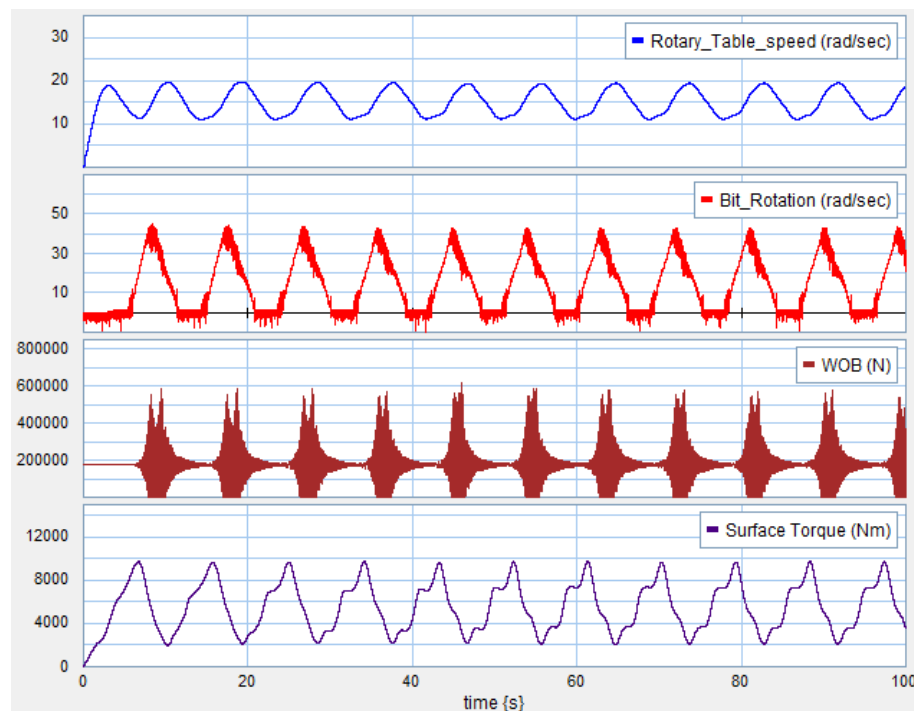


Figure 12: Torsional spring-damper system unable to eliminate stick-slip and bit-bounce vibrations at 15 rad/sec (142 rpm) table speed and 175 kN WOB

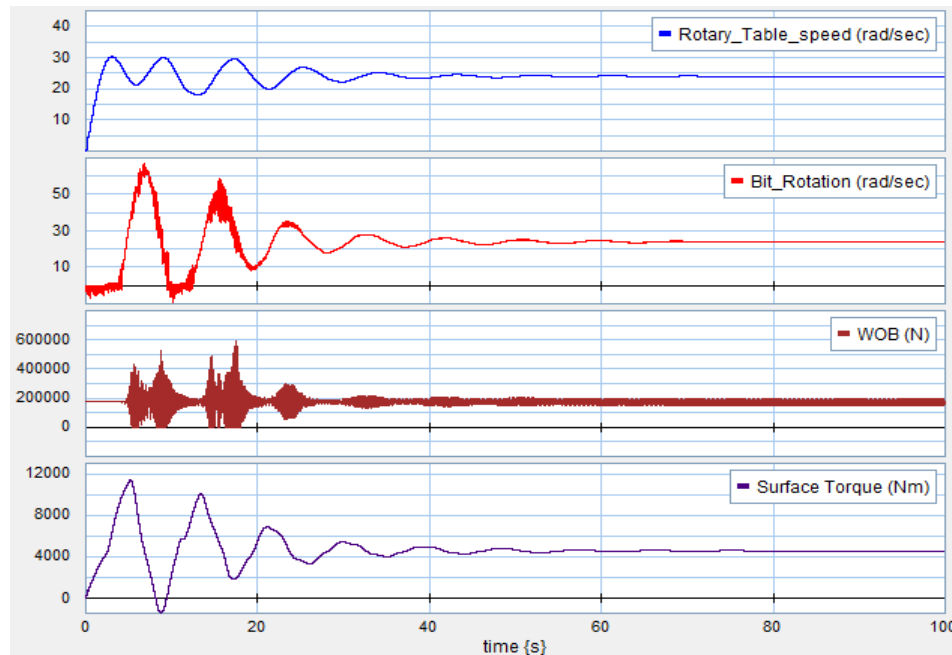


Figure 13: Stick-slip and bit-bounce vibrations eliminated by torsional spring-damper system at 24 rad/sec (230 rpm) table speed and 175 kN applied WOB

VI. ADVANTAGES OF LQR CONTROLLER

Stick-slip occurs at a rotary speed below a certain threshold value. Fig. 14 shows the threshold phenomena of stick-slip vibrations. The threshold value depends on system parameters such as design of the drillstring, mud, bit, BHA and weight on bit (WOB). Fig. 15 and 16 show the threshold rotary speed for different applied WOB for conventional drilling, drilling with torsional spring-damper system near the

rotary table, and drilling with the LQR controller. Simulation results show that for a particular applied WOB the LQR controller gives the lowest magnitude of the threshold rotary speed. At higher WOB the difference in the threshold rotary speed between the LQR controller and torsional spring-damper system increases, and it indicates that at higher WOB, and notwithstanding certain practical implementation issues to be discussed later, an LQR controller can increase the no stick-slip zone significantly compared to a torsional spring-damper system.

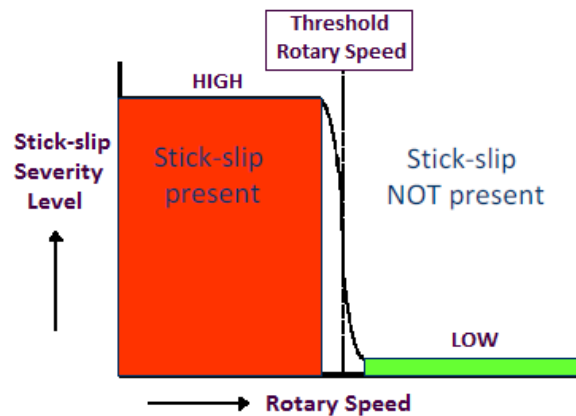


Figure 14: Threshold speed for stick-slip vibration

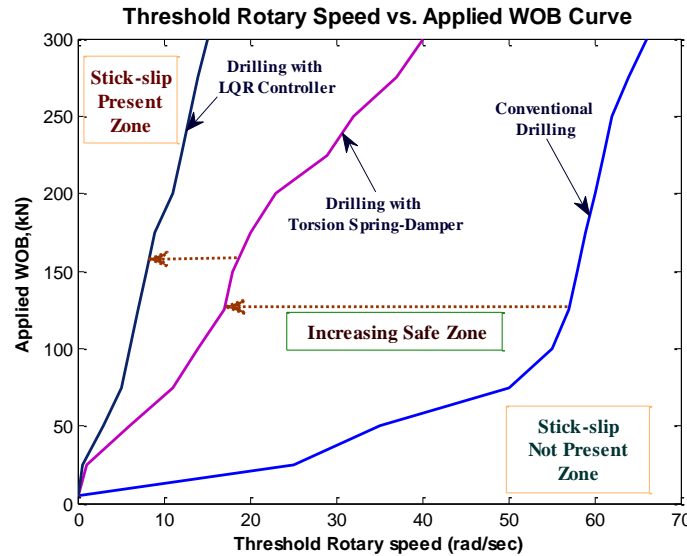


Figure 15: Threshold rotary speed vs. applied WOB curve for different operating conditions at 2200 m depth.

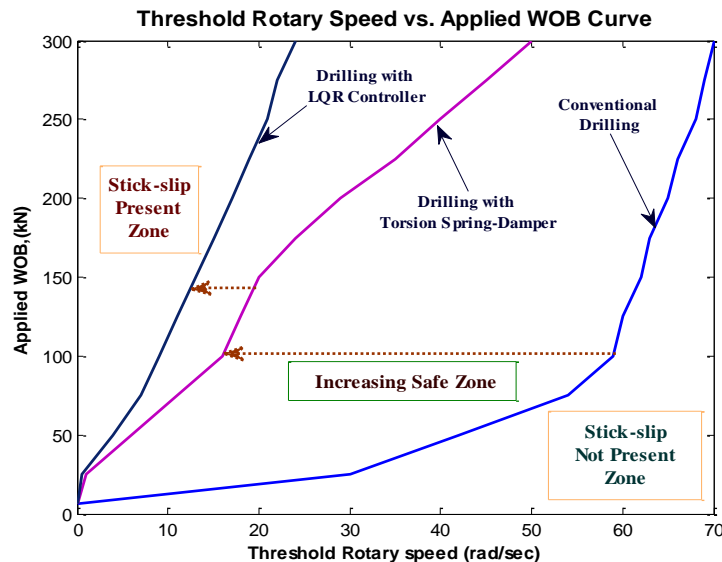


Figure 16: Threshold rotary speed vs. applied WOB curve for different operating conditions at 4200 m depth.

During drilling, the LQR controller requires: (i) motor current, (ii, iii) rotary table rotary speed and displacement, (iv-v) bit rotary speed and displacement. Except for the bit speed and displacement, all other quantities in the controller can be measured. The bit speed measurement (and calculation of bit rotary displacement through integration) requires downhole equipment that is expensive and at this point not typically used in well drilling because the information is not needed if a controller is not used. Bit speed

measurement is the biggest challenge preventing LQR and other sophisticated controller implementations, as discussed also in [2-3, 19]. The virtual spring-damper of the STRS system requires only measurement of motor current, giving it an economic and implementation advantage at present. The additional potential benefits of LQR are expected to motivate drillers to eventually use advanced downhole measurement tools, to enable such control. The

additional cost of instrumentation would be justified by even smoother drilling and fewer tool failures.

VII. CONCLUSIONS

Development and application of a bond graph model of a drillstring using a lumped segment approach has been presented. The proposed dynamic model includes the mutual dependence of axial and torsional vibrations, and coupling between axial and torsional vibration due to bit-rock interaction. While the top drive motor dynamics assume a DC motor, the bond graph formalism allows for easy substitution of an AC or hydraulic motor submodel (all three types are in common use in the drilling industry). Use of a different type of motor would require rederiving the LQR matrices and gains; however, the procedure outlined herein would still apply. Simulation results show the same qualitative trends as field observations regarding stick-slip oscillations and their relationship to rotary speed, weight on bit, and bit bounce. These vibrations are self excited, and they generally disappear as the rotary speed is increased beyond a threshold value and the applied weight on bit decreases. However, increasing rotary speed may cause lateral problems and decreasing applied weight on bit decreases rate of penetration. The model also includes a state feedback controller that was designed based on a linear quadratic regulator (LQR) technique. It has been shown that self-excited stick-slip oscillations in oilwell drillstrings are largely suppressed by the application of LQR control. Therefore, it is possible to drill smoothly at very low speeds which are otherwise not possible without LQR control. It has been shown that the advantages of using LQR control increase with higher applied WOB. The performance of LQR control for mitigation of stick-slip decreases with increasing depth. It nonetheless retains an advantage compared to a system with a spring-damper isolator. This should motivate the use of LQR controllers in future when practical challenges in measuring required state variables for LQR control are addressed by advances in downhole measurement technology. The implementation of the high-order model in commercial software that allows block diagrams to be superimposed on bond graphs greatly facilitated inclusion of the coupled axial and torsional degrees of freedom due to bit-rock interaction, along

with the controller. The simulation time is very fast compared to high order finite-and discrete-element models, making the model suitable as a tool for design and sensitivity analysis.

REFERENCES

- [1] Sarker, M.M., Rideout, D.G., & Butt, S.D. (2012) "Dynamic Model of an Oilwell Drillstring with Stick-Slip and Bit-Bounce Interaction" Submitted to 10th International Conference on Bond Graph Modeling and Simulation. Genoa, Italy, July 8-11, 2012. The Society for Modeling and Simulation International, San Diego, CA, USA.
- [2] Leine, R. I., Van Campen, D. H., & Keultjes, W. J. G. (2002). Stick-slip Whirl Interaction in Drillstring Dynamics. *Journal of Vibration and Acoustics*, 124(2), 209–220.
- [3] Yigit, A. S., & Christoforou, A. P. (2000). Coupled Torsional and Bending Vibrations of Actively Controlled Drillstrings. *Journal of Sound Vibration*, 234(1), 67–83.
- [4] Yigit, A. S., & Christoforou, A. P. (2006). Stick-slip and Bit-bounce Interaction in Oil-well Drillstrings. *Journal of Energy Resources Technology*, 128(4), 268–274.
- [5] Richard, T., Gernay, C., & Detournay, E. (2004). Self-excited Stick-slip Oscillations of Drill Bits. *Comptes Rendus – Mecanique*, 332(8), 619–626.
- [6] Richard, T., Gernay, C., & Detournay, E. (2007). A Simplified Model to Explore the Root Cause of Stick-slip Vibrations in Drilling Systems with Drag Bits. *Journal of Sound and Vibration*, 305(3), 432–456.
- [7] Sampaio, R., Piovan, M.T. and Lozano, G.V. (2007). Coupled axial torsional vibrations of drillstring by means of nonlinear model. *Journal of Mechanics Research Communications*. 34, 497–502.
- [8] Navarro-Lopez, E.M. and Cortes, D. (2007). Avoiding Harmful Oscillations in a Drillstring through Dynamical Analysis. *Journal of Sound and Vibrations*. 307,152–171.
- [9] Zamanian, M., Khadem, S.E. and Ghazavi, M.R. (2007). Stick-slip oscillations of drag bits by considering damping of drilling mud and active damping system. *Journal of Petroleum Science Engineering*. 59(3–4), 289–299.
- [10] Khulief, Y. A., Al-Sulaiman, F. A., & Bashmal, S. (2007). Vibration Analysis of Drillstrings with Self-excited Stick-slip Oscillations. *Journal of Sound and Vibration*, 299(3), 540–558.
- [11] Cobern, M. E., & Wassell, M. E. (2004). Drilling Vibration Monitoring and Control System. National Gas Technologies II Conference Phoenix, AZ, 8-11 February.
- [12] Eronini, I. E., Somerton, W. H., & Auslander, D. M. (1982). A Dynamic Model for Rotary Rock Drilling. *Journal of Energy Resources Technology*, 104(2), 108–120.

- [13] Karnoop, D. C., Margolis, D. L., & Rosenberg, R. C., (1999). *System Dynamics; Modeling and Simulation of Mechatronics Systems*, 3rd ed., John Wiley & Sons, Inc., New York.
- [14] Karkoub, M., Zribi, M., Elchaar, L., & Lamont, L. (2010). Robust μ -Synthesis Controllers for Suppressing Stick-slip Induced Vibrations in Oil Well Drill Strings. *Multibody System Dynamics*, 23(2), 191–207.
- [15] Serrarens, A. F. A., van de Molengraft, M. J. G., Kok, J. J., & van den Steen, L. (1998). H_∞ Control for Suppressing Stick-slip in Oil Well Drillstrings. *Control Systems, IEEE*, 18(2), 19–30.
- [16] Karkoub, M., Abdel-Magid, Y. L., & Balachandran, B. (2009). Drill-string Torsional Vibration Suppression Using GA Optimized Controllers. *Journal of Canadian Petroleum Technology*, 48(12), 32–38.
- [17] Canudas-de-Wit, C., Rubio, F. R., & Corchero, M. A. (2008). D-OSKIL: A New Mechanism for Controlling Stick-slip Oscillations in Oil Well Drillstrings. *IEEE Transactions on Control Systems Technology*, 16(6), 1177–1191.
- [18] Pavkovic, D., Deur, J., & Lisac, A. (2011). A Torque Estimator-based Control Strategy for Oil-well Drill-string Torsional Vibrations Active Damping Including an Auto-tuning Algorithm. *Control Engineering Practice*, 19(8), 836–850.
- [19] Puebla, H., & Alvarez-Ramirez, J. (2008). Suppression of Stick-slip in Drillstrings: A Control Approach Based on Modeling Error Compensation. *Journal of Sound and Vibration*, 310(4-5), 881–901.
- [20] Womer, K. A., Torkay, D. R., Villanueva, G. P., Geehan, T., Brakel, J., Pirovolou, D., et al. (2011). Results of July 15, 2010 IADC Stick-Slip Mitigation Workshop. *SPE/IADC Drilling Conference and Exhibition. Amsterdam, The Netherlands: Society of Petroleum Engineers*.
- [21] <http://www.softorque.com>
- [22] Kriesels, P. C., Keultjes, W. J. G., Dumont, P., Huneidi, I., Owoeye, O. O., & Hartmann, R. A. (1999). Cost Savings through an Integrated Approach to Drillstring Vibration Control. *SPE/IADC Middle East Drilling Technology Conference. Abu Dhabi, United Arab Emirates: Society of Petroleum Engineers*.

APPENDIX A

AN OVERVIEW OF BOND GRAPH FORMALISM

Bond graph is an explicit graphical tool for capturing the energetic structure of a physical system and uniquely suited to the understanding of physical system dynamics. Because of the ability to provide concise description of complex systems the bond graph formulation can be used in hydraulics, mechatronics, thermodynamic and electric systems. The bond graph language expresses a general class of physical systems through power (effort and flow) interactions and the factors of power have different interpretations in different physical domains.

Table A1 expresses the generalized power (effort and flow) variables and energy (momentum and displacement) variables in some physical domains. The generalized inertias and capacitance in bond graph [13] store energy as a function of the system state variables, the sources provide inputs from the environment, and the generalized resistors remove energy from the system. The state variables are generalized momentum and displacement for inertias and capacitances, respectively. Where the time derivatives of generalized momentum p and displacement q are generalized effort e and flow f . The power-conserving elements allow changes of state to take place. Such elements include power-continuous generalized transformer (TF) and gyrator (GY) elements that algebraically relate elements of the effort and flow vectors into and out of the element. In certain cases, such as large motion of rigid bodies in which coordinate transformations are functions of the geometric state, the constitutive laws of these power-conserving elements can be state modulated. Dynamic force equilibrium and velocity summations in rigid body systems are represented by power-conserving elements called 1 and 0 junctions, respectively.

Table A1: Generalized bond graph quantities

Variable	General	Translation	Rotation
Effort	$e(t)$	Force	Torque
Flow	$f(t)$	Velocity	Angular Velocity
Momentum	$p = \int e dt$	Linear momentum	Angular momentum
Displacement	$q = \int f dt$	Displacement	Angular displacement
Energy	$E(p) = \int^p f dp$ $E(q) = \int^q e dq$	Kinetic potential	Kinetic Potential

Table A2: Bond graph elements

	SYMBOL	CONSTITUTIVE LAW (LINEAR)	CAUSALITY CONSTRAINTS		SYMBOL	CONSTITUTIVE LAW (LINEAR)	CAUSALITY CONSTRAINTS
SOURCES				2-PORT ELEMENTS			
Flow	Sf \longleftarrow	$f = f(t)$	fixed flow out	Transformer	$\begin{array}{c} 1 \longleftarrow \text{TF} \longrightarrow 2 \\ n \end{array}$	$e_2 = n e_1$ $f_1 = n f_2$	effort in – effort out, or flow in – flow out
Effort	Se \longrightarrow	$e = e(t)$	fixed effort out				
ENERGETIC ELEMENTS							
Inertia	\longrightarrow I	$f = \frac{1}{I} \int e dt$	preferred integral	Modulated Transformer	$\begin{array}{c} 1 \longleftarrow \text{MTF} \longrightarrow 2 \\ \downarrow \theta \\ n(\theta) \end{array}$	$e_2 = n(\theta) e_1$ $f_1 = n(\theta) f_2$	
	\longleftarrow I	$e = I \frac{df}{dt}$			Gyrator	$\begin{array}{c} 1 \longleftarrow \text{GY} \longrightarrow 2 \\ n \end{array}$	$e_2 = n f_1$ $e_1 = n f_2$
Capacitor	\longleftarrow C	$e = \frac{1}{C} \int f dt$	preferred integral	Modulated Gyrator	$\begin{array}{c} 1 \longleftarrow \text{MGY} \longrightarrow 2 \\ \downarrow \theta \\ n(\theta) \end{array}$	$e_2 = n(\theta) f_1$ $e_1 = n(\theta) f_2$	
	\longrightarrow C	$f = C \frac{de}{dt}$					
Resistor	\longleftarrow R	$e = Rf$	none	CONSTRAINT NODES			
	\longrightarrow R	$f = \frac{1}{R} e$		1-junction	$\begin{array}{c} 1 \longleftarrow 1 \longrightarrow 2 \\ \swarrow \searrow \\ \sqrt{3} \end{array}$	$e_2 = e_1 - e_3$ $f_1 = f_2$ $f_3 = f_2$	one flow input

APPENDIX B

EQUATIONS USED IN THE MODEL

FLUID DRAG FORCE/DAMPING FOR AXIAL MODEL

Assuming the nonlaminar Newtonian flow formulations and ignoring any eccentric location of the drillstring in the wellbore, the pressure drop in the annulus between the borehole and a stationary drillpipe can be written as below [12]

$$\Delta P = \frac{\alpha_a \rho_m Q^2 dx}{4 \pi^2 (r_w - r_o) (r_w^2 - r_o^2)^2}$$

(B1)

The resulting longitudinal force, F_A (positive down) exerted on the drillstring segment which is moving with velocity, V_n can be written as below [12]

$$F_A = - \left\{ \frac{\alpha_a \rho_m \pi (r_w + r_o) dx}{4} \right\} \left[\frac{Q}{\pi (r_w^2 - r_o^2)} \right] + V_n \left\{ \left[\frac{Q}{\pi (r_w^2 - r_o^2)} \right] + V_n \right\}$$

(B2)

And the drag force on the drillstring due to flow in the drillpipe is given by [12]

$$F_p = - \left\{ \frac{\alpha_p \rho_m \pi r_i dx}{4} \right\} \left[\frac{Q}{\pi r_i^2} - V_n \right] \left\{ \frac{Q}{\pi r_i^2} - V_n \right\}$$

(B3)

FLUID FRICTION RESISTANCE/VISCOUS DAMPING TO ROTATION

Again ignoring any nonconcentric drillpipe location in the borehole, a simple expression for the fluid torque is given by [4, 12]

$$T_{R_n} = \left(\frac{2 \pi \mu_e r_o^3}{r_w - r_o} \right)_n dx_n \omega_n$$

(B4)

APPENDIX C

ROTARY DRILLING SIMULATION MODEL AND DATA

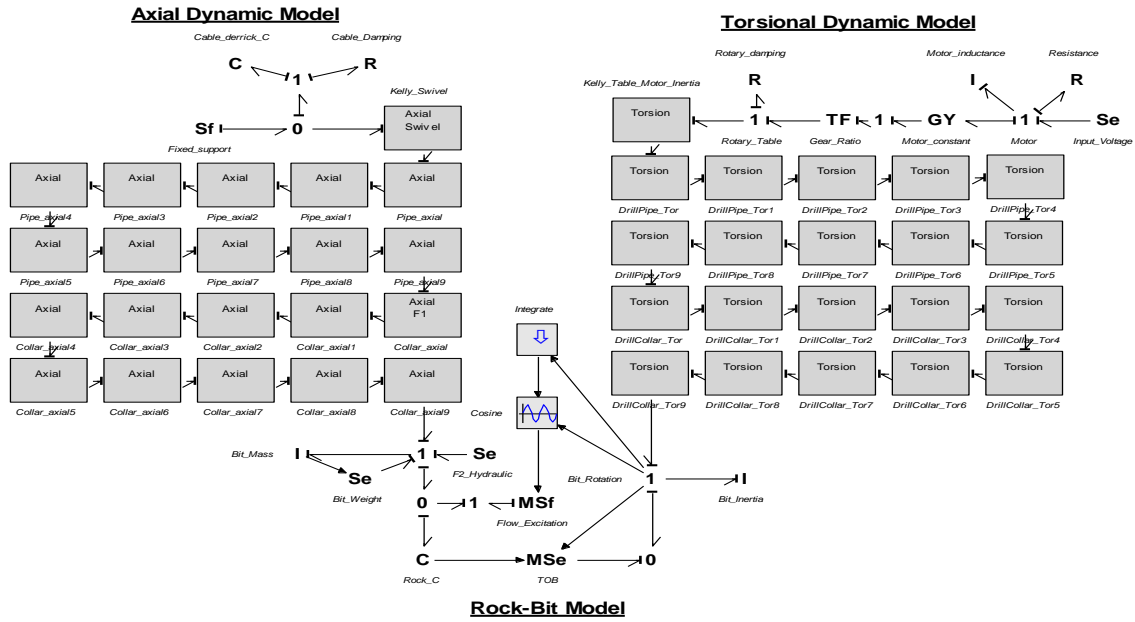


Figure C1: Bond graph model of rotary drilling system

Table C1: Data used in rotary drilling simulation

Drillstring data	
Cable and derrick spring constant	9.3e+06 N/m
Swivel and derrick mass	7031 kg
Kelly length	15 m
Kelly outer diameter	0.379 m
Kelly inner diameter	0.0825 m
Drill pipe length	2000 m
Drill pipe outer diameter	0.101 m (4 in)
Drill pipe inner diameter	0.0848 m (3.34 in)
Drill collar length	200 m
Drill collar outer diameter	0.171 m (6.75 in)
Drill collar inner diameter	0.0571 m (2.25 in)
Drill string material	Steel
Wellbore diameter	0.2 m
Drill bit-rock data	
Bit type	PDC (Single cutter)
Drill bit diameter	0.2 m (7.875 in)
Drill bit mass	65 kg
Rock stiffness	1.16e+09 N/m
Rock damping	1.5e+05 N.sec/m
Surface elevation amplitude s_0	0.001
Bit factor, b	1
Cutting coefficient ξ, C_1, C_2	1, 1.35e-08, -1.9e-4
Frictional coefficient $\mu_0, \alpha, \beta, \gamma$ & ν	0.06, 2, 1, 1 & 0.01
Threshold force, W_{fs}	10000 N
Hydraulic data	
Mud fluid density	1198 kg/m ³
Mud flow rate, Q	$Q_m + Q_g \sin(qt)$
Mean mud flow rate, Q_m	0.022 m ³ /sec
Mud flow pulsation amplitude, Q_g	0.002 m ³ /sec
Freq. of variation in mud flowrate, q	25.13 rad/sec
Equivalent fluid viscosity for fluid resistance to rotation μ_e	30e-03 Pa.sec
Weisbach friction factor outside drill pipe or collar, α_g	0.045
Weisbach friction factor inside drill pipe or collar, α_p	0.035
Motor data	
L, K_m , n and R_m	0.005 H, 6 V/s, 7.2 and 0.01 Ω